10542 *Biochemistry* **2009,** *48,* 10542–10548
DOI: 10.1021/bi901131u

BIOCHEMISTRY
including biophysical chemistry & molecular biology
Article

Ring1B Contains a Ubiquitin-Like Docking Module for Interaction with Cbx Proteins[†,‡]

Irina Bezsonova,[§,∥] John R. Walker,[§,⊥] John P. Bacik,[§,⊥] Shili Duan,[∥] Sirano Dhe-Paganon,*[,§] and Cheryl H. Arrowsmith*[,§,∥]

[§] *Structural Genomics Consortium, University of Toronto, 101 College Street, Toronto, Ontario, M5G 1L5, Canada, and* [∥] *Ontario Cancer Institute and Department of Medical Biophysics, University of Toronto, 101 College Street, Toronto, Ontario M5G 1L7, Canada.* [⊥] *These authors made equal contributions to the manuscript.*

Received July 3, 2009; Revised Manuscript Received September 30, 2009

ABSTRACT: Polycomb group (PcG) proteins are a special set of repressive transcription factors involved in epigenetic modifications of chromatin. They form two functionally distinct groups of catalytically active complexes: Polycomb repressive complex 1 (PRC1) and 2 (PRC2). The PRC1 complex is an important yet poorly characterized multiprotein histone ubiquitylation machine responsible for maintaining transcriptionally silent states of genes through histone H2A K119 modification. The Ring domain containing subunits of PRC1 also have substrate-targeting domains that interact with Cbx proteins, which have been implicated in chromatin and RNA binding. In this work, we present a high resolution structure of the C-terminal domain of Ring1B, revealing a variant ubiquitin-like fold with a distinct conserved surface region. On the basis of crystal structure and mutational analysis of this domain we show that the conserved surface is responsible for interaction with Cbx members of the PRC1 and homodimer formation. These data suggest a mechanism by which Ring1B serves as an adaptor that mediates binding between the members of the PRC1 complex and the nucleosome.

The genome is organized into areas that are accessible for transcriptional activity and areas that are transcriptionally silent; this patterning is governed by chromatin modifications in part catalyzed by a set of repressive transcription factors called Polycomb group (PcG[1]) proteins (*1*, *2*). They form at least two functionally distinct groups of catalytically active protein complexes: Polycomb repressive complex 1 (PRC1) and 2 (PRC2). PRC1 has E3 ubiquitin ligase activity that ubiquitylates histone H2A at K119 (*3*). PRC2 has methyltransferase activity for histone H3 at K27 (*4*). Both complexes are conserved from plants to human and found primarily associated with heterochromatin, where they contribute to the maintenance of transcriptional silencing and to the maintenance of cellular identity.

Polycomb silencing in *Drosophila* is associated with three important events: (1) methylation of histone H3 at position K27 (H3K27) by PRC2, (2) recognition of the methylated H3K27 mark by the CHROMO domain of PC within PRC1, and (3) ubiquitylation of histone H2A at K119 mediated by Ring proteins of PRC1 leading to gene silencing (*5*). Although the molecular mechanism by which ubiquitylation causes transcriptional silencing is not well understood, it has been proposed that ubiquitylated histones directly interfere with transcriptional machinery (*6*).

Drosophila PRC1 is composed of at least four principal components, including two Ring domain containing proteins (dRING and PSC), a CHROMO domain containing protein (PC), and a SAM domain containing protein (PH). Mammals have multiple paralogues of dRING and PSC (Ring1A, Ring1B, and Pcgf1,2,3,4,5,6, respectively), CHROMO proteins (Cbx2,4,6,7,8), and SAM domain containing proteins (Phc1,2,3). How, when, and where these multiple subunits mix and match to participate in specific complexes and chromatin regulatory functions remains unclear (*7*, *8*).

The structural and quaternary organization of Polycomb multiprotein complexes and their mechanism of action remains poorly understood. The structure of a principal component of PRC2, Eed, in complex with a peptide derived from Ezh2, has been determined (pdbID 2QXV), revealing the molecular basis of the specific recognition of Ezh2 by Eed required for PRC2 histone methyltransferase activity (*9*). The Ring domains of Ring1B and Bmi1 form a heterodimer within PRC1 that is necessary for full catalytic activity and may form a scaffold for other components to bind (*10*, *11*). For example, the C-terminal domain of Ring1B interacts with Cbx proteins, which in turn bind to methylated histone tails and small RNAs (*7*). In 2008, a detailed sequence analysis of the C-terminal domain of the PRC1 Ring proteins revealed weak (< 10%) but statistically significant sequence similarity between this region and ubiquitin (*12*). This domain (named RAWUL for Ring finger and WD40 associated ubiquitin-like) is of particular interest because it is important for targeting PRC1 E3 ubiquitin ligase activity to the nucleosome, likely through a direct interaction with a Cbx subunit of PRC1.

[†] The Structural Genomics Consortium is a registered charity (no. 1097737) that receives funds from the Canadian Institutes for Health Research, the Canadian Foundation for Innovation, Genome Canada through the Ontario Genomics Institute, GlaxoSmithKline, Karolinska Institutet, the Knut and Alice Wallenberg Foundation, the Ontario Innovation Trust, the Ontario Ministry for Research and Innovation, Merck & Co., Inc., the Novartis Research Foundation, the Swedish Agency for Innovation Systems, the Swedish Foundation for Strategic Research and the Wellcome Trust. This research was supported in part by the Canadian Cancer Society. CHA holds a Canada Research Chair in Structural Proteomics. Use of the Advanced Photon Source was supported by the U.S. Department of Energy, Office of Science, Office of Basic Energy Sciences, under contract no. DE-AC02-06CH11357.

[‡] The atomic coordinates have been deposited in the Protein Data Bank (PDB, http://www.rcsb.org/): 3H8H.

*To whom correspondence should be addressed. Phone: 1(416) 946-3876 (S.D.P.); 1(416) 946-0881 (C.H.A.). Fax: 1(416) 946-0880. E-mail: sirano.dhepaganon@utoronto.ca (S.D.P.); carrow@uhnreserch.ca (C.H.A.).

[1] Abbreviations: PcG, Polycomb group; PRC1, PRC2, Polycomb repressive complex 1 and 2; C-Ring1B, C-terminal domain of Ring1B; UBL, ubiquitin-like domain; NMR, nuclear magnetic resonance.

 Published on Web 09/30/2009

Recent attempts to structurally characterize the C-terminal domain of Ring1B (C-Ring1B) show that it exists in equilibrium between monomer and dimer states in solution with a dissociation constant, K_d, of approximately 200 μM, as shown by NMR, ITC, and analytical gel filtration (*13*, *14*). It has also been shown using surface plasmon resonance that the C-Ring1B binds tightly to the C-terminal region of Cbx2,4,6,7, and 8 with a K_d varying from 9.2 nM for Cbx7 to 180 nM for Cbx6 and Cbx8 (*14*, *15*). In addition, analytical ultracentrifugation studies of C-Ring1B and its complex with Cbx7 showed that the C-Ring1B/Cbx7 interaction prevents C-Ring1B dimer formation (*14*, *15*).

We sought to determine how the C-terminal domain of Ring1B interacts with Cbx-proteins in PRC1. Here we report the crystal structure of the RAWUL domain, showing that it corresponds to variants of the ubiquitin fold family that share a conserved protein−protein interaction surface distinct from that of ubiquitin. We show that the mutation of Tyr 262 residing in the center of this conservative surface patch to Ala disrupts the UBL domain binding to Cbx7. The same surface also mediates homotypic interactions within the crystal and is conserved among all human PRC1 Ring proteins, suggesting a possible mechanism for homo- and heterodimerization among Ring proteins and a probable mode of interaction with Cbx proteins.

MATERIALS AND METHODS

DNA Constructs. DNA fragments encoding full length Ring1B and full length Cbx7 were obtained from the mammalian gene collection (MGC 13490 and 54332, respectively). The Ring1B C-terminal domain region was amplified using PCR and cloned into pET28MHL vector (GenBank accession EF456735). Resulting plasmids encoded N-terminal His-tag, followed by a TEV cleavage site and residues 200−330/200−336/220−330/220−336 of Ring1B. Region 209−251 of Cxb7 was cloned into pET28-MHL vector, similar to Ring1B.

Protein Expression and Purification. *Escherichia coli* (DE3) Codon Plus cells were used for overexpression of Ring1B and Cbx7 constructs. Ring1B and Cbx7 constructs were grown in either LB medium to yield unlabeled protein or minimal medium M9 SeMet High-Yield growth media kit (Medicilon) to yield Se-Met labeled protein. Cells transformed with Ring1B and Cbx7 plasmids were grown in minimal medium M9 enriched with ^{15}N ammonium chloride, which yielded $^{15}N/^{1}H$ labeled proteins for NMR purposes. Typically, cells were grown at 37 °C to OD_{600} = 1.0 and induced at 15 °C for 10 h with 1 mM IPTG. In some cases, Se-Met was added to the minimal media an hour prior to IPTG induction. After sonication, His-tagged Ring1B proteins were purified using Talon beads (Clontech) followed by TEV cleavage and HiLoad Superdex 75 size exclusion chromatography (GE Healthcare). Cbx7 was purified from the insoluble fraction of cell lystate in 6 M guanidine HCl. After metal affinity column purification, Cbx7 was refolded in the presence of equimolar amounts of C-terminal domain of Ring1B by fast dilution. SeMet-labeled and native Ring1B (res. 220−330) were crystallized in 2 M ammonium sulfate, 2% PEG 400, 0.1 M HEPES, pH 7.5 at 18 °C. Crystals were obtained using the hanging-drop technique, cryoprotected by immersion into 15% glycerol, 2 M ammonium sulfate, 2% PEG 400, 0.1 M HEPES, pH 7.5, and frozen by immersion into liquid nitrogen.

Crystallographic Data Collection, Structure Solution, and Refinement. Data from crystals of a selenomethionine derivative of the Ring1B (res. 220−330) were collected on beamline 19-ID of the Advanced Photon Source at the selenium peak wavelength and processed using the HKL-2000 program suite (*16*). Solve and Resolve were used to locate the selenium substructure and to build the initial model (*17*). A native data set was collected on a home-source Rigaku FR-E and used for the final refinement of the structure. Automatic model building using ARP/wARP (*18*) was followed by iterative manual model building aided by the graphics program Coot (*19*) and TLS and restrained refinement using REFMAC (*20*), leading to a final model with an R_{work} of 0.20 and an R_{free} of 0.24 for data from 28.27 to 2.10 Å. Initial parameters for TLS refinement were obtained from the TLSMD server (*21*, *22*).

Circular Dichroism. Protein solutions for CD analysis were dialyzed against 25 mM phosphate, pH 7.5, 150 mM NaCl. CD experiments were performed on AVIV 62DS CD spectrophotometer. Far-UV spectra of 3 μM solutions of each, the WT and the Y262A, were collected at 25 °C between 199.5 and 260 nm (1 nm bandwidth) in 0.5 nm steps using a cell with a path length of 0.1 cm. The molar ellipticity, [Θ], was calculated using the following equation

$$[\Theta] = \frac{\Theta}{c \times l \times 10 \times n}, \ [\text{degrees} \cdot \text{cm}^2 \cdot \text{dmol}^{-1}]$$

where Θ is measured ellipticity, c is molar concentration of protein, l is path length in cm, and n is the number of amino acid residues in the protein.

Thermal Melts. Differential scanning fluorescence (DSF) (*23*) was used to monitor unfolding transitions of the WT and the Y262A mutant using a real time PCR instrument "LightCycler 480II" from Roche. Sypro Orange fluorescence dye (Invitrogen) was added to the 0.1 and 0.2 mg/mL solutions of each WT and mutant proteins, and the fluorescence was monitored between temperatures of 20 and 95 at 1 °C intervals with heating rate of 1 °C/min. The excitation wavelength of 456 nm and emission wavelength of 580 nm were used. The T_m value was estimated as the midpoint of transition between the folded and unfolded states of the protein using the sigmoid Boltzmann function.

NMR Experiments. All NMR experiments were carried out at the Bruker Avance 600 MHz spectrometer equipped with cryoprobe at 25 °C. All of the NMR samples were prepared with a buffer containing 20 mM Tris, pH 8.0, 500 mM NaCl, and 500 mM imodazole. The final NMR samples contained 0.3 mM protein/complex, 90% H_2O and 10% D_2O. $^{15}N/^{1}H$ HSQC experiments were utilized to monitor binding of Cbx7 to the WT and Y262A mutant of Ring1B (residues 220−330). Because Cbx7 peptide was not soluble in water, it was dissolved in 6 M guanidine HCl and then refolded in the presence of the ^{15}N labeled Ring1B using fast dilution method. The spectra were processed with NMRPipe software (*24*) and analyzed with nmrView program (*25*).

RESULTS AND DISCUSSIONS

Ring1B C-Terminal Domain is Ubiquitin-Like. Previous characterization of the conserved C-terminal region of the Ring1B suggested that the region consists of two small subdomains connected by a long variable linker, both of which were required for efficient Cbx binding (*14*). To define the boundaries of the C-terminal domain of Ring1B, we have designed multiple DNA constructs for bacterial protein expression and have assessed the expression and solubility of the proteins. In total, 13 expression constructs of the region were made including

Table 1: Data Collection, Phasing, and Refinement Statistics[a]

	selenomethionine derivative	native
PDB Code		3H8H
space group	$P6_522$	$P6_522$
unit cell, Å	$a = b = 72.36$, $c = 91.08$	$a = b = 72.17$, $c = 90.97$
beamline	APS 19ID	FR-E
wavelength, Å	0.97935	1.54178
resolution	50−2.1	30−2.1
unique reflections	15273	8680
data redundancy	11.4 (11.1)	14.4 (8.8)
completeness, %	99.7 (99.6)	100 (100)
I/sig$I$	25.7 (3.15)	33.8 (3.8)
R_{sym}[c]	0.14 (0.86)	0.11 (0.60)
Phasing		
no. of Selenium Sites	8	
mean figure of merit	0.20	
overall Z-score from SOLVE	19.1	
Refinement		
resolution		2.1−28.3
reflections used		8213
all atoms, including solvent		831 {84}
R_{work}/R_{free}, %[b]		19.7/24.5
rmsd bond length, Å		0.02
rmsd bond angle, deg		1.8
figure of merit		0.85
mean B value, Å^2		20.62
MolProbity Ramachandran Analysis		
favored, %		98.84
allowed, %		100
disallowed, %		0

[a]Highest resolution shell is shown in parentheses. [b]R_{free} value was calculated with 5% of the data. [c]$R_{sym} = 100 \times \sum(|I - \langle I\rangle|)/\sum(\langle I\rangle)$, where I is the observed intensity and $\langle I\rangle$ is the average intensity from multiple observations of symmetry-related reflections.

residues in the region 200−336. Of these, four constructs, 200−330, 200−336, 220−330, and 220−336, were soluble and expressed well. They were then used for crystallization and NMR experiments. The construct containing residues 220−330 yielded the best diffracting crystals, which were used for structure determination.

The crystal structure of Ring1B (220−330) was solved using a selenomethionine derivative, and a native data set was then refined to 2.1 Å resolution. The final model comprising 747 protein atoms and 84 solvent atoms, exhibits excellent stereochemistry with no Ramachandran violations as judged by PROCHECK and the MolProbity Ramachandran Plot (*26*, *27*). Details of data collection and refinement are shown in Table 1, and a ribbon diagram of the refined C-Ring1B domain is shown in Figure 1A. The C-terminal domain of Ring1B has a ubiquitin-like fold consisting of five β-strands, two α-helices, and a 3-residue 3_{10} helical turn, arranged in order $\beta1$, $\beta2$, $\alpha1$, 3_{10}, $\beta3$, $\beta4$, $\alpha2$, and $\beta5$, where the strands form a single β-sheet. The surface of the domain contains significant positive charges and two hydrophobic patches on the opposite sides of the domain (Figure 2A). Residues 273−284, whose sequence is not conserved among Ring1A/1B/Pcgf, are not visible in the electron density and are presumably flexible or disordered. Thus, these residues appear to form a variable internal loop (as opposed to previous suggestions that they link two separate domains (*14*) and may contribute to specific functions of the Ring1B RAWUL domain among the PRC1 Ring proteins.

Structure-based comparison of Ring1B with ubiquitin (Figure 1B,C) shows that while the overall fold of the RAWUL domain is similar (rmsd of 2.1 Å for Cα atoms compared to human ubiquitin, PDB: 1UBQ), there are also several distinct features. First, α1 helix is one helical turn longer in Ring1B than in ubiquitin. Second, there is a long flexible loop and a 3_{10} helical turn preceding the $\beta3$ strand that is missing in ubiquitin. Third, the 3-residue 3_{10} helix in ubiquitin is extended into a two-turn α-helix, α2, in Ring1B. Finally, a characteristic feature of the RAWUL domain is a gap between the long α1 helix and $\beta2$ strand in Ring1B (Figure 1B), resulting in a surface lined with aromatic and aliphatic side chains (Y262, L269, I248) and capped at one end by a positive charge (R266, R246). Ubiquitin interacts with a set of ubiquitin-like proteins through the characteristic Ile44-centered saddle-point. The analogous region of Ring1B does not form a groove and has a significantly different charge distribution. Together, these differences suggest that ubiquitin binding targets are distinct from those of Ring1B.

The RAWUL Domain Shares Unique Features with a Subset of Other Ubiquitin-Like Domains. Ubiquitin-like domains (*28*) (UBLs) can be divided into two distinct groups, modifiers and nonmodifiers. Proteins belonging to the first group, including ubiquitin, SUMO, and Nedd8, act as post-translational modifiers that are activated by E1 ligases through a thiol-ester bond between the terminal glycine carboxyl and a conserved cysteine in E2 proteins and subsequently transferred to the ε-amino group of substrate lysines by E3 ligases. Nonmodifying ubiquitin-like domains are often part of larger proteins and are found in over 80 human genes, many of which are themselves E3 ligases.

Using the DALI server (*29*), we performed a search of the PDB for domains with structural similarity to the Ring1B RAWUL domain, identifying 151 nonredundant structures with similarity Z-scores greater than 2 (Supporting Information Table S1). The domains with the closest matches include both ubiquitin modifiers and nonmodifiers. Hits with highest Z-scores are ubiquitin-like modifiers that include human γ-aminobutyric acid receptor-associated protein-like 1 (GABARAP1), microtubule-associated protein 1 light chain 3 (MAPLC3), yeast autophagy protein 8 (Atg8), and bovine GATE16. These proteins are involved in the autophagy system and in intracellular vesicle trafficking (*30*). Their mature forms have a conserved C-terminal Gly residue that is used for covalent substrate modification in a manner similar to ubiquitylation. Unlike ubiquitin, however, autophagy substrates include membrane lipids. A hallmark of autophagy UBLs is an additional helical element N-terminal to the ubiquitin-like fold. Interestingly, these proteins share with the RAWUL domain the characteristic opening between the $\beta2$ and $\alpha1$ elements. For several of the top DALI hits, structures are available for the protein complexed to its binding partner including Atg8/Atg19, GABARAP/calreticulin, and SUMO/PIASX complexes. Remarkably, the majority of these UBLs bind their partners via the $\beta2/\alpha1$ region. These UBL-binding peptides bind in an extended conformation, forming a β-strand, and extend the UBL's β-sheet. Thus, the widened $\beta2/\alpha1$ opening appears to be a conserved protein−protein interaction surface and may play a similar role in Ring1B.

Among nonmodifying proteins with close structural similarity to the Ring1B RAWUL domain, several are E3 ligases, including

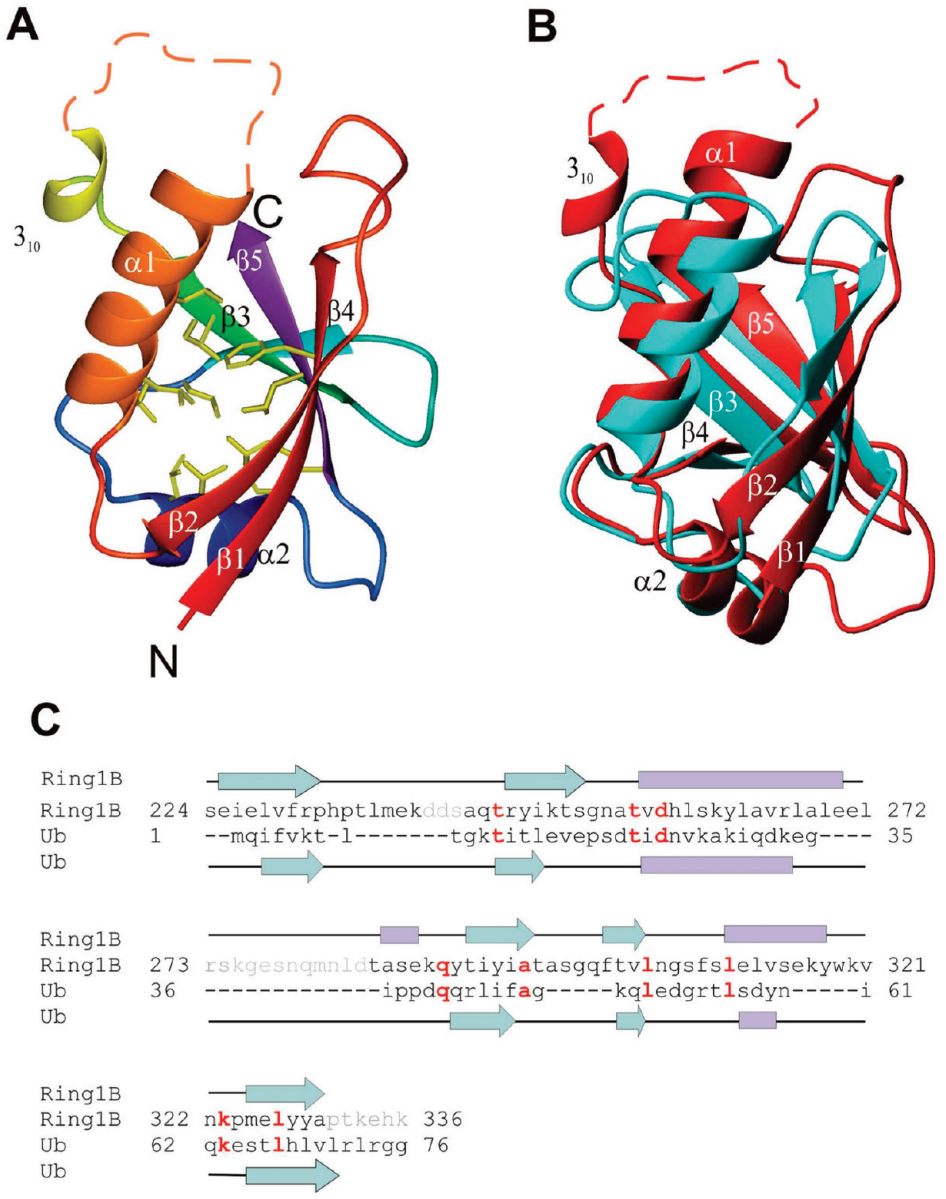

FIGURE 1: Structure of the Ring1B RAWUL domain. (A) The backbone structure is represented in ribbon format with rainbow colors. Residues 273−284, missing in the crystal structure, are shown as a dotted line. Secondary structure elements and N- and C-termini are labeled. Side chains of residues L228, F230, V256, L259, L263, L305, L311, V314, L327, and M325 forming the hydrophobic core of the domain are shown as yellow sticks. The backbone structures of the RAWUL domain and ubiquitin (shown as red and cyan ribbons, respectively) are compared in (B), where the two proteins are superimposed. (C) Structure-based sequence alignment of the RAWUL domain and ubiquitin. Identical residues are shown in red.

UHRF1 (*31*), which ubiquitylates histone H3, and Parkin (*32*), which ubiquitylates cytoskeletal proteins (*32*). Interestingly, the UBLs of these proteins also share the widened opening between β2 and α1 elements. Often, nonmodifying UBL domains serve as protein−protein interaction modules (*28*), consistent with the role of the Ring1B RAWUL domain in binding to several proteins involved in PRC1 complex formation and histone ubiquitylation.

RAWUL Domain Binding to Cbx7. Residues that are conserved are usually functionally important. We therefore mapped conserved residues in Ring1B, Ring1A, Pcgf1,2,3,4,5, and 6 onto the surface of the Ring1B RAWUL domain (Figure 3). Remarkably, highly conserved residues are clustered exclusively on the surface of the α1/β2 region. This strongly suggests that the conserved surface is important for interactions common for all RAWUL-containing proteins in the PRC1 complex such as dimerizaton and/or substrate binding.

A number of potential binding partners have been identified for Ring1B (*33*). Of these, three are involved in PRC1 complex formation: Bmi1, Cbx7, and Phc2. Bmi1 interacts through the N-terminal Ring1B Ring domain (*10*, *11*), and Cbx7 and Phc2 were proposed to bind to the C-terminal region of Ring1B. The region of Phc2 that interacts with Ring1B is not known. However, the hydrophobic C-terminal region of Cbx7, which is conserved among Cbx7, 2, 4, 6, and 8 and termed the C-box, has been implicated in high affinity binding to C-Ring1B with K_d ranging from 9.2 to 180 nM as measured using the surface plasmon resonance method (*14*).

To test our hypothesis that conserved residues clustered on the surface of the Ring1B UBL domains (Figure 3) are important for Ring1B/Cbx complex formation, we have mutated the residue

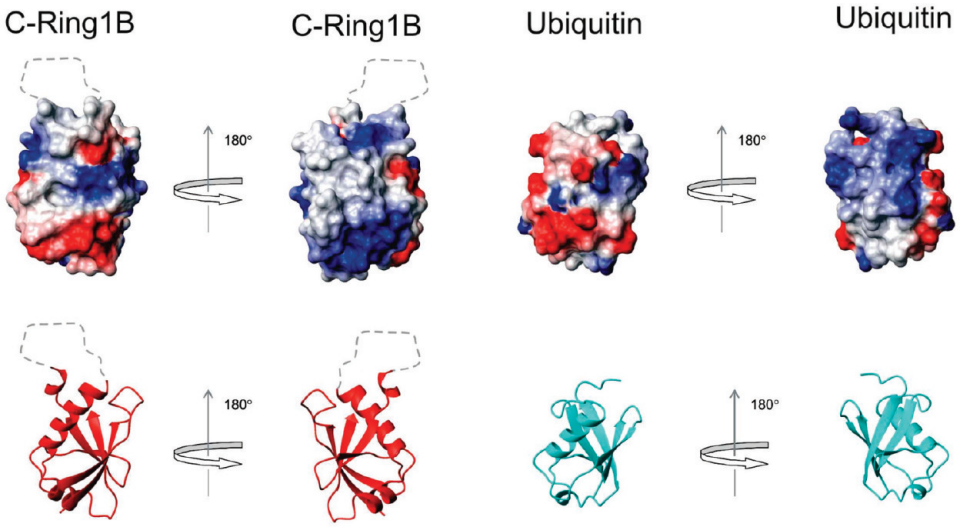

FIGURE 2: Surface representation of the Ring1B RAWUL domain (A) and ubiquitin (B) colored by electrostatic potential; negative charges are shown in red, positive in blue, and uncharged surface is white. Both proteins are shown in two orientations rotated by 180° with respect to each other. Ribbon representations of the proteins are shown in the lower panel for clarity. Residues 273−284 missing in the crystal structure are shown as a dotted line.

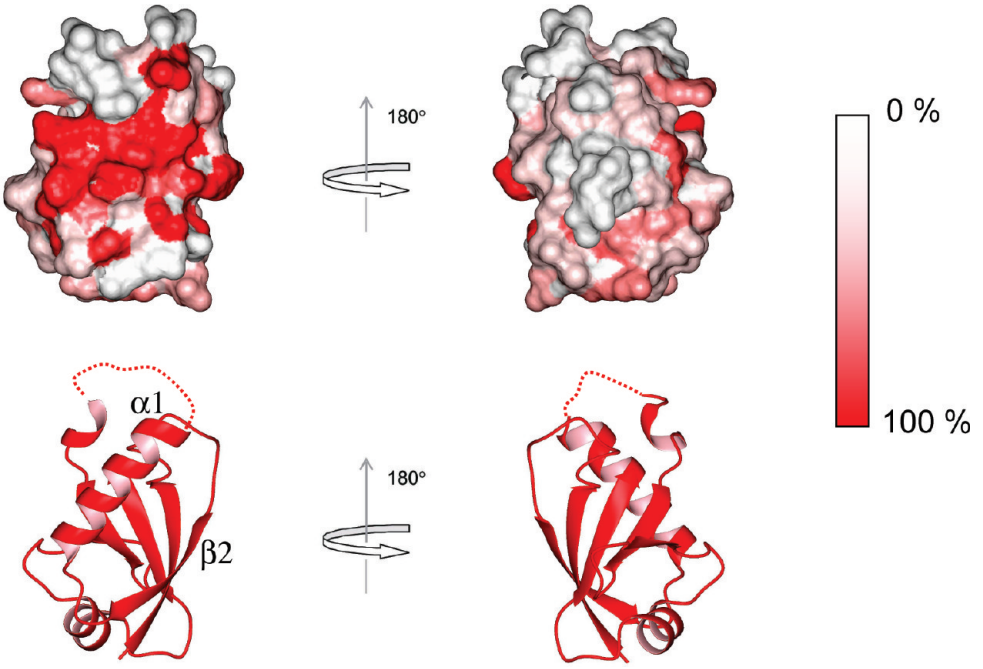

FIGURE 3: Surface conservation among PRC1 Ring proteins. The surface of the RAWUL domain of Ring1B is colored from white to red by degree of amino acid residue conservation in Ring1B, Ring1A, Pcgf1,2,3,4,5, and 6 (*12*). The domain is shown in two orientations rotated by 180° with respect to each other, and the ribbon diagram of the domain with labeled α1 and *β*2 elements is shown in the lower panel for clarity.

Tyr 262 located in the center of the conserved surface patch to Ala and evaluated the effect of this mutation on Ring1B binding to Cbx7 peptide using heteronuclear NMR spectroscopy. The $^{15}N/^{1}H$ HSQC spectra of free ^{15}N-labeled WT and Y262A UBL domains (Figure 4, black) were compared to those recorded in the presence of the unlabeled Cbx7 peptide (Figure 4, red). It is clear from Figure 4 that the WT UBL domain binds to Cbx7 peptide at equimolar ratio, leading to significant chemical shift changes and peak broadening in the spectrum. In contrast, the spectrum of the Y262A mutant reveals no chemical shift changes in the presence of Cbx7. Thus, the Y262A mutation compromises the Ring1B binding to Cbx7.

To ensure that the Y262A mutation does not significantly alter either the structure or stability of the domain leading to its failure to bind the Cbx7 peptide as observed by NMR, we have performed circular dichroism and differential scanning fluorescence based thermal melt experiments for both the WT and the Y262A mutant. The Far UV CD spectra yielded identical spectra for both domains (Supporting Information Figure S1), which indicates that the structure of the domain remains largely unaltered by the Y262A mutation. The stabilities of the two domains are also very similar, with the melting temperatures (T_m) of 66.0 ± 1.3 °C for the WT and 63.8 ± 0.4 °C for the Y262A mutant. Thus, Tyr 262 mutation impairs the Ring1B binding to Cbx7, supporting the conclusion that the conserved surface region of the Ring1B UBL domain is involved in Cbx7 binding.

It has been recently shown that the C-terminal region of Ring1B forms a homodimer in solution with K_d of ~200 μM

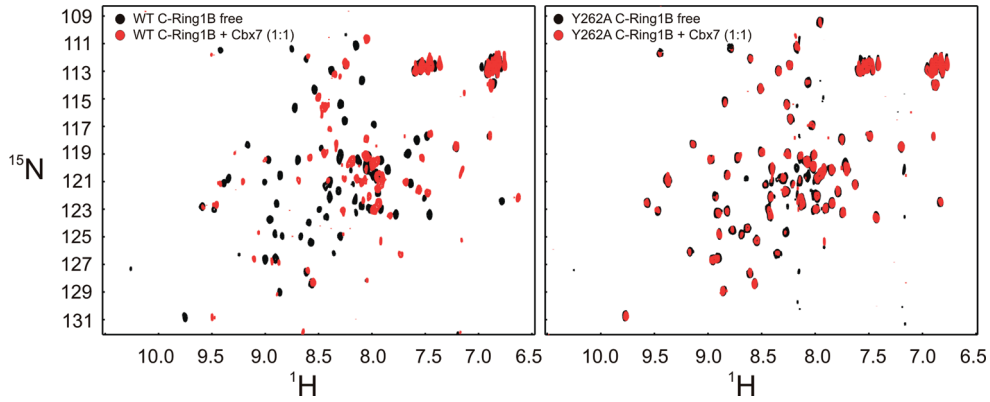

FIGURE 4: On the left, $^{15}N/^{1}H$ HSQC spectra of ^{15}N-labeled Ring1B (residues 220−330) in the absence (black) and the presence (red) of unlabeled Cbx7 peptide (residues 209−251). The molar ratio of Ring1B to Cbx7 is 1:1. On the right, $^{15}N/^{1}H$ HSQC spectra of the ^{15}N-labeled Y262A mutant of the Ring1B (residues 220−330) in the absence (black) and the presence (red) of equimolar concentration of the unlabeled Cbx7.

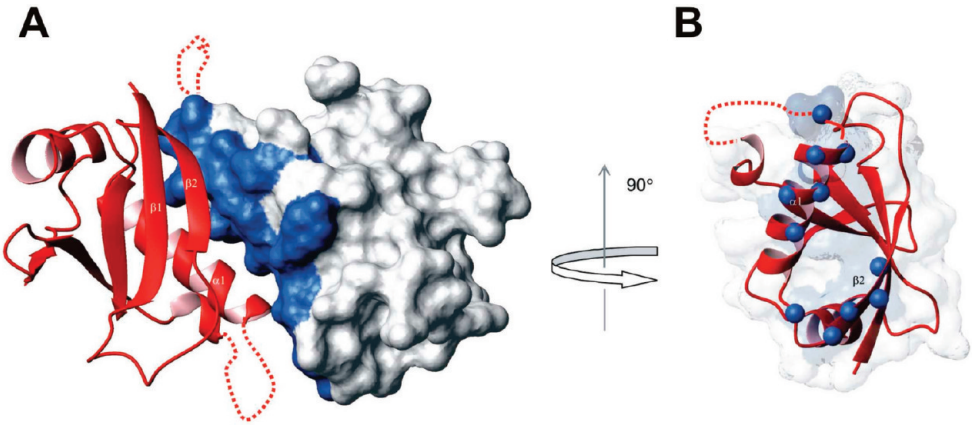

FIGURE 5: Structure of the Ring1B RAWUL domain's dimer. The amino acid residues forming the dimerization interface are colored in blue on the surface of the domain (A). Their Cα atoms are shown as blue balls in the ribbon representation of the RAWUL domain in (B), where the domain is rotated by 90° with respect to (A).

as determined by NMR, ITC, and analytical gel filtration (*13*, *14*). Notably, analytical ultracentrifugation studies show that the dimer formation is precluded by C-Ring1B binding to Cbx7 peptide (K_d of 9.2 nM) (*13*, *14*). Crystal contact analysis can be used to establish the mode of domain dimerization. Although the RAWUL domain crystallized in a space group with one molecule per asymmetric unit, the analysis using the PISA (protein interfaces, surfaces, and assemblies) database (*34*) reveals one symmetry-related interface with a buried surface area of 596 A^2 per molecule (Figure 5). Notably, this interface involves predominantly the same α1 and β2 elements and overlaps significantly with the proposed Cbx-binding site. This result, together with the fact that Cbx7 binding to the C-Ring1B prevents dimerization of the UBL domain, implies that RAWUL domains and Cbx members of the PRC1 complex may compete for the same binding site on the surface of the UBL domain, potentially providing the means for reorganization and activation of the PRC1 complex.

CONCLUSIONS

The PRC1 complex is an important yet poorly characterized multiprotein histone ubiquitylation machine responsible for maintaining transcriptional silencing through histone H2A K119 modification. We have determined the structure of the C-terminal region of the Ring1B subunit of PRC1 and identified its interaction interface with another PRC1 subunit, Cbx7, responsible for specific nucleosome recognition and PRC1 targeting to its substrate, histone H2A. The structure presented here has a single conserved α1/β2 surface coincident with similar protein−protein interaction surfaces in a subset of ubiquitin-like domains. We have shown that this surface is involved in two competing processes: dimerization of the UBL domain and its binding to Cbx7. Because the dimerization interface is conserved in the other RAWUL-containing subunits of PRC1, this raises the possibility of hetero-oligomerizaton between RAWUL containing PRC1 proteins. For the case of the Ring1B interaction with Cbx7, the heterotypic interaction is stronger than Ring1B homodimerization (K_d of 9.2 nM versus 200 μM, respectively), as shown by previous surface plasmon resonance, analytical ultracentrifugation, NMR, ITC, and analytical gel filtration studies (*13*, *14*). However, the relative interaction affinities for other RAWUL and Cbx combinations are not known. That putative quaternary interactions and Cbx-binding mediated by the α1/β2 surface are mutually exclusive may have important functional consequences. Identification of the RAWUL-Cbx C-box interaction surface provides a foundation to dissect the potential role of the RAWUL domains as central adaptors of PRC1 to mediate interactions with chromatin.

ACKNOWLEDGMENT

We are grateful to George Avvakumov and Mani Ravichandran for useful discussions and suggestions. We thank Nataliya

Nady and Guillermo Senisterra for their help with CD and fluorescence data acquisition and analysis.

SUPPORTING INFORMATION AVAILABLE

WT and Y262A C-Ring1B far UV CD spectra and the table of known domains structurally similar to the C-Ring1B as found by Dali server (also available at http://pubs.acs.org.myaccess.library.utoronto.ca). This material is available free of charge via the Internet at http://pubs.acs.org.

REFERENCES

1. Schwartz, Y. B., and Pirrotta, V. (2008) Polycomb complexes and epigenetic states. *Curr. Opin. Cell. Biol. 20*, 266–273.
2. Shukla, A., Chaurasia, P., and Bhaumik, S. R. (2009) Histone methylation and ubiquitination with their cross-talk and roles in gene expression and stability. *Cell. Mol. Life Sci. 66*, 1419–1433.
3. Wang, H., Wang, L., Erdjument-Bromage, H., Vidal, M., Tempst, P., Jones, R. S., and Zhang, Y. (2004) Role of histone H2A ubiquitination in Polycomb silencing. *Nature 431*, 873–878.
4. Kuzmichev, A., Nishioka, K., Erdjument-Bromage, H., Tempst, P., and Reinberg, D. (2002) Histone methyltransferase activity associated with a human multiprotein complex containing the Enhancer of Zeste protein. *Genes Dev. 16*, 2893–2905.
5. Cao, R., Tsukada, Y., and Zhang, Y. (2005) Role of Bmi-1 and Ring1A in H2A ubiquitylation and Hox gene silencing. *Mol. Cell 20*, 845–854.
6. Zhou, W., Zhu, P., Wang, J., Pascual, G., Ohgi, K. A., Lozach, J., Glass, C. K., and Rosenfeld, M. G. (2008) Histone H2A monoubiquitination represses transcription by inhibiting RNA polymerase II transcriptional elongation. *Mol. Cell 29*, 69–80.
7. Bernstein, E., Duncan, E. M., Masui, O., Gil, J., Heard, E., and Allis, C. D. (2006) Mouse polycomb proteins bind differentially to methylated histone H3 and RNA and are enriched in facultative heterochromatin. *Mol. Cell. Biol. 26*, 2560–2569.
8. Vincenz, C., and Kerppola, T. K. (2008) Different polycomb group CBX family proteins associate with distinct regions of chromatin using nonhomologous protein sequences. *Proc. Natl. Acad. Sci. U.S.A. 105*, 16572–16577.
9. Han, Z., Xing, X., Hu, M., Zhang, Y., Liu, P., and Chai, J. (2007) Structural basis of EZH2 recognition by EED. *Structure 15*, 1306–1315.
10. Buchwald, G., van der Stoop, P., Weichenrieder, O., Perrakis, A., van Lohuizen, M., and Sixma, T. K. (2006) Structure and E3-ligase activity of the Ring−Ring complex of polycomb proteins Bmi1 and Ring1b. *EMBO J. 25*, 2465–2474.
11. Li, Z., Cao, R., Wang, M., Myers, M. P., Zhang, Y., and Xu, R. M. (2006) Structure of a Bmi-1-Ring1B polycomb group ubiquitin ligase complex. *J. Biol. Chem. 281*, 20643–20649.
12. Sanchez-Pulido, L., Devos, D., Sung, Z. R., and Calonje, M. (2008) RAWUL: A new ubiquitin-like domain in PRC1 ring finger proteins that unveils putative plant and worm PRC1 orthologs. *Bmc Genomics 9*, 308–318.
13. Czypionka, A., de los Panos, O. R., Mateu, M. G., Barrera, F. N., Hurtado-Gomez, E., Gomez, J., Vidal, M., and Neira, J. L. (2007) The isolated C-terminal domain of Ring1B is a dimer made of stable, well-structured monomers. *Biochemistry 46*, 12764–12776.
14. Wang, R. J., Ilangovan, U., Robinson, A. K., Schirf, V., Schwarz, P. M., Lafer, E. M., Demeler, B., Hinck, A. P., and Kim, C. A. (2008) Structural transitions of the RING1B C-terminal region upon binding the polycomb cbox domain. *Biochemistry 47*, 8007–8015.
15. Schoorlemmer, J., MarcosGutierrez, C., Were, F., Martinez, R., Garcia, E., Satijn, D. P. E., Otte, A. P., and Vidal, M. (1997) Ring1A is a transcriptional repressor that interacts with the Polycomb-M33 protein and is expressed at rhombomere boundaries in the mouse hindbrain. *EMBO J. 16*, 5930–5942.
16. Minor, W., Cymborowski, M., and Otwinowski, Z. (2002) Automatic system for crystallographic data collection and analysis. *Acta Phys. Pol., A 101*, 613–619.
17. Terwilliger, T. C. (2003) SOLVE and RESOLVE: automated structure solution and density modification. *Methods Enzymol. 374*, 22–37.
18. Cohen, S. X., Ben Jelloul, M., Long, F., Vagin, A., Knipscheer, P., Lebbink, J., Sixma, T. K., Lamzin, V. S., Murshudov, G. N., and Perrakis, A. (2008) ARP/wARP and molecular replacement: the next generation. *Acta Crystallogr., Sect. D: Biol. Crystallogr. 64*, 49–60.
19. Emsley, P., and Cowtan, K. (2004) Coot: model-building tools for molecular graphics. *Acta Crystallogr., Sect. D: Biol. Crystallogr. 60*, 2126–2132.
20. Winn, M. D., Murshudov, G. N., and Papiz, M. Z. (2003) Macromolecular TLS refinement in REFMAC at moderate resolutions. *Methods Enzymol. 374*, 300–321.
21. Painter, J., and Merritt, E. A. (2006) TLSMD web server for the generation of multi-group TLS models. *J. Appl. Crystallogr. 39*, 109–111.
22. Painter, J., and Merritt, E. A. (2006) Optimal description of a protein structure in terms of multiple groups undergoing TLS motion. *Acta Crystallogr., Sect. D: Biol. Crystallogr. 62*, 439–450.
23. Lo, M. C., Aulabaugh, A., Jin, G., Cowling, R., Bard, J., Malamas, M., and Ellestad, G. (2004) Evaluation of fluorescence-based thermal shift assays for hit identification in drug discovery. *Anal. Biochem. 332*, 153–159.
24. Delaglio, F., Grzesiek, S., Vuister, G. W., Zhu, G., Pfeifer, J., and Bax, A. (1995) NMRPipe: a multidimensional spectral processing system based on UNIX pipes. *J. Biomol. NMR 6*, 277–293.
25. Johnson, B. A. (2004) Using NMRView to visualize and analyze the NMR spectra of macromolecules. *Methods Mol. Biol. 278*, 313–352.
26. Davis, I. W., Leaver-Fay, A., Chen, V. B., Block, J. N., Kapral, G. J., Wang, X., Murray, L. W., Arendall, W. B.III, Snoeyink, J., Richardson, J. S., and Richardson, D. C. (2007) MolProbity: all-atom contacts and structure validation for proteins and nucleic acids. *Nucleic Acids Res. 35*, W375–W383.
27. Davis, I. W., Murray, L. W., Richardson, J. S., and Richardson, D. C. (2004) MOLPROBITY: structure validation and all-atom contact analysis for nucleic acids and their complexes. *Nucleic Acids Res. 32*, W615–W619.
28. Jentsch, S., and Pyrowolakis, G. (2000) Ubiquitin and its kin: how close are the family ties? *Trends Cell Biol. 10*, 335–342.
29. Holm, L., Kaariainen, S., Rosenstrom, P., and Schenkel, A. (2008) Searching protein structure databases with DaliLite v.3. *Bioinformatics 24*, 2780–2781.
30. Cecconi, F., and Levine, B. (2008) The role of autophagy in mammalian development: cell makeover rather than cell death. *Dev. Cell 15*, 344–357.
31. Hashimoto, H., Horton, J. R., Zhang, X., and Cheng, X. (2009) UHRF1, a modular multidomain protein, regulates replication-coupled crosstalk between DNA methylation and histone modifications. *Epigenetics 4*, 8–14.
32. Moore, D. J. (2006) Parkin: a multifaceted ubiquitin ligase. *Biochem. Soc. Trans. 34*, 749–53.
33. Neira, J. L., Roman-Trufero, M., Contreras, L. M., Prieto, J., Singh, G., Barrera, F. N., Renart, M. L., and Vidal, M. (2009) The Transcriptional Repressor RYBP Is a Natively Unfolded Protein Which Folds upon Binding to DNA (dagger). *Biochemistry 48* (6), 1348–1360.
34. Krissinel, E., and Henrick, K. (2007) Inference of macromolecular assemblies from crystalline state. *J. Mol. Biol. 372*, 774–797.